Progress In Electromagnetics Research C, Vol. 129, 1–15, 2023

A Radar Waveform Design of MCPC Method for Interrupted Sampling Repeater Jamming Suppression via Fractional Fourier Transform

Ji Li, Junjie Zhou, Wei Wang*, and Min Liu

Abstract—Interrupted Sampling Repeater Jamming (ISRJ) is an electronic countermeasure against radar echo signals that generates many false targets to mask the real target echoes, which seriously affects radar target detection performance. Most of the ISRJ suppression methods require accurate estimation of the signal parameters, and the estimation methods are complex. Based on the characteristics of discontinuous ISRJ sampling and orthogonality between multi-carrier phase coding (MCPC) signal's subcarriers, we propose a method for ISRJ identification and suppression based on an improved MCPC signal. By analyzing the pulse compression of the echo, we found that different types of intermittent sampling interference have different peaks after pulse compression. Based on this feature, we introduce Fractional Fourier Transform to filter out interference. Theoretical analysis and simulation results show that the method can effectively suppress the three classical ISRJ interferences. The method suppresses ISRJ during echo processing without any parameter estimation for real scenes and has stronger robustness than other existing schemes.

1. INTRODUCTION

With the continuous development of modern electronic countermeasures technology, the signal jamming technology for military radar has been constantly improved, among which the interrupted-sampling and repeater jamming (ISRJ) based on Digital Radio Frequency Memory (DRFM) technology has been widely used in radar signal jamming. The interference strategy was first proposed by Wang et al. [1] and Sparrow and Cikalo [2], respectively. Since the intercepted signals are part of radar signals, coherent false targets will be generated after pulse compression [3]. At present, the typical ISRJ styles mainly include interrupted-sampling and direct repeater jamming (ISDJ)[1], interrupted-sampling and periodic repeater jamming (ISPJ) [4], and interrupted-sampling and cyclic repeater jamming (ISCJ) [5].

In order to eliminate ISRJ, many scholars have made unremitting efforts. [6] proposes a deep learning network recognition and suppression method for ISRJ. [8] proposes an adaptive anti-ISRJ interference method based on compressed sensing (CS). [9] proposes a one-dimensional half-parameter method. [10] adopts the sliding window pulse compression method. In [12], an interference suppression method based on the idea of "reconstruction and elimination" is proposed. Papers [11, 21, 24] encode the signal in time domain and frequency domain within and between pulses to enhance the overall correlation of the signal and reduce the correlation of fragments, so as to achieve the purpose of suppressing ISRJ. In [7, 13], the design method of waveform and mismatch filter is proposed. The optimization criteria are established through specific situations, and different optimization algorithms are used to jointly optimize the waveform parameters and adaptive filter to suppress ISRJ. In [14], an iterative algorithm

Received 20 October 2022, Accepted 29 December 2022, Scheduled 20 January 2023
* Corresponding author: Wei Wang (wangwei@csust.edu.cn).
The authors are with the College of Computer and Communication Engineering, Changsha University of Science & Technology, Changsha 410000, China.

of wideband radar based on filter is proposed. The algorithm constructs max-TF function according to the time-frequency (TF) energy distribution of [15], which can automatically and accurately extract non-interference segments and generate a bandpass filter to suppress ISRJ interference. Based on the discontinuous nature of ISRJ signals in the time domain, compressed perception-related studies have also been applied to the reconstruction of real targets [16]. Based on the aggregation characteristics of linear frequency modulation (LFM) signals in the fractional domain, [17, 18] use fractional Fourier transform (FRFT) to construct the sparsity of signals, so as to suppress ISRJ interference. In [19], an anti-intermittent sampling interference method based on LFM piecewise pulse compression is proposed. The piecewise LFM signal is used as the impulse response signal of matched filter, and the narrowband filter bank is constructed. The orthogonality between the piecewise LFM signals is used to effectively suppress the interference. Based on the analysis of the cross-ambiguity function of ISRJ, [20] proposes an ISRJ recognition method based on Doppler compensation.

The above methods can effectively fight against ISRJ, but they also have some disadvantages. For example, they need too much computation and have poor real-time performance; the effect of suppressing ISRJ is too dependent on parameter estimation; and they are limited to a specific ISRJ. In addition, the existing anti-intermittent sampling interference technology mainly uses LFM signal, while the research on using MCPC signal to do intermittent sampling interference waveform is less. Compared with LFM signal, MCPC signal has better low interception performance, higher pulse compression gain, and other good properties. At present, the research on anti-ISRJ of MCPC signal is mainly from the perspective of waveform design, while the research on anti-ISRJ of other aspects of MCPC signal is rare. Based on the above analysis, we want to suppress ISRJ from the perspective of waveform design and echo signal processing. We propose an FRFT filtering method combined with waveform design to resist intermittent sampling interference.

Based on MCPC signal, we propose an ISRJ-resistant waveform, namely, SCC-MCPC (SubCarrier Cover Multicarrier Chaotic Phase Code) signal, which is encoded in time domain by chaotic two-phase coding for each orthogonal frequency division multiplexing (OFDM) signal chip and then obtained by intercepting code chips of equal length with different subcarriers. On the basis of this signal, we propose an anti-intermittent sampling interference method based on FRFT [22, 23] subsection filtering pulse compression. This method performs fractional Fourier transform on the signal under the set optimal rotation order, performs filtering processing interference and target discrimination and screening under the optimal rotation order, removes the interference detected in the echo, and uses the echo signal after removing the interference to do pulse compression processing on the matched signal to achieve the purpose of suppressing ISRJ. The simulation results show that the proposed method can effectively suppress the three ISRJ signals, and the comparison experiments prove the superiority of the method.

The simulation results show that the proposed method can effectively suppress the three ISRJ signals. Finally, the simulation results prove the superiority of this method.

2. SCC-MCPC SIGNAL MODEL

MCPC-OFDM signal has ideal ambiguity function, high target resolution, and good detection capability. MCPC radar signal combines multi-carrier phase-coding with orthogonal frequency division multiplexing signal, which has excellent ambiguity function performance, pulse compression performance, and low interception performance. It not only has the advantages of OFDM signal such as good anti-fading ability, large time bandwidth product and high frequency spectrum utilization, but also has the advantages of orthogonality of chaotic sequences and large number of generation and different lengths. SCC-MCPC signal is based on MCPC signal and introduces the idea of subcarrier mutual cover. From the perspective of signal structure, it is obtained by intercepting fixed length of each subcarrier. Because of the discontinuous nature of intermittent interference sampling, it is always impossible to completely sample all subcarrier signals, and different subcarriers are mutually orthogonal, so no matter how to sample in the time domain, the orthogonality between subcarriers can always be used to remove the sampled signal segment, so that the signal can effectively suppress ISRJ interference.

The complex envelope of SCC-MCPC-OFDM signal can be described as:

$$\begin{aligned} s(t) &= \sum_{n=1}^{P} w_n \exp(j2\pi f_n t)\mu(t) \\ &= \sum_{n=1}^{P}\sum_{m=1}^{M} w_n a_{n,m} \exp(j2\pi f_n t)\mu(t) \\ &= \sum_{n=1}^{P}\sum_{m=1}^{M} w_n a_{n,m} \exp(j2\pi f_n t)\mathrm{rect}(t-(m-1)t_b)\mathrm{rect}(t-(n-1)t_B) \end{aligned} \tag{1}$$

$$\mathrm{rect}(t) = \begin{cases} 1, & 0 \le t \le t_b \\ 0, & \text{else} \end{cases} \tag{2}$$

where P represents the number of subcarriers, M the number of subcarrier chips, $\mu(t)$ the complex envelope of subcarrier, $w_n = |w_n| e^{j\varphi_{n,m}}$ the amplitude and phase weighting coefficient of the nth subcarrier, $a_{n,m} = \exp(j\varphi(n,m)t)$ the chaotic phase coding value on the mth chip of the subcarrier, $f_n = (n-1)\Delta f$ the carrier frequency of the nth subcarrier, $\Delta f = \frac{1}{t_b}$ the subcarrier frequency interval, t_b the duration of a single chip, $t_B = M * t_b$. Represents the duration of each subcarrier. The iteration expression of logistic chaotic code is $x_{k+1} = 1 - 2x_k^2$, and chaotic attraction domain is $x_k \in [-1, 1]$ m. By selecting the process variable x_k, the corresponding chaotic sequence can be generated according to the mapping expression. The generated chaotic sequences need to be quantized and coded. Quantitative rules can be described as:

$$a_n = 2\pi \cdot ceil(N_P x_p + 0.5)/N_P \tag{3}$$

According to the quantization rules, through the different values of N_P, we can get two phase codes and different polyphase codes. Here, $N_P = 2$ is selected to represent chaotic two-phase coding. $\{a_1, a_2, a_3, \ldots, a_{M\times N}\}$ is the final binary coded sequence after binary quantization, where E_k is the mean of the original mixed sequence, and E_k can be described as:

$$E_k = \frac{\sum_{i=1}^{M*N} x_i}{N * M} \tag{4}$$

The chaotic phase coding value of the mth chip on the nth subcarrier can be described as:

$$a_{n,m} = \begin{cases} -1, & x_i \le E \\ 1, & x_i > E_k \end{cases} \tag{5}$$

The echo signal $s_R(t)$ of the scattering target at distance R is described as:

$$\begin{aligned} s_R(t) &= As(t-\Delta t) \\ &= A\sum_{n=1}^{P} w_n \exp(j2\pi f_n(t-\Delta t))\mu(t-\Delta t) \\ &= A\sum_{n=1}^{P}\sum_{m=1}^{M} w_n a_{n,m} \exp(j2\pi f_n(t-\Delta t))\mu(t-\Delta t) \\ &= A\sum_{n=1}^{P}\sum_{m=1}^{M} w_n a_{n,m} \exp(j2\pi f_n(t-\Delta t))\mu_n(t-\Delta t)\,\mu_m(t-\Delta t) \\ &= A\sum_{n=1}^{P}\sum_{m=1}^{M} w_n a_{n,m} \exp(j2\pi f_n(t-\Delta t)\mathrm{rect}(t-\Delta t-(m-1)t_b)\mathrm{rect}(t-\Delta t-(n-1)t_B) \end{aligned} \tag{6}$$

where $\Delta t = \frac{2R}{c}$ is the echo time delay, A the echo amplitude, and c the propagation speed of light in the air. The time-frequency structure of SCC-MCPC signal is shown in Fig. 1.

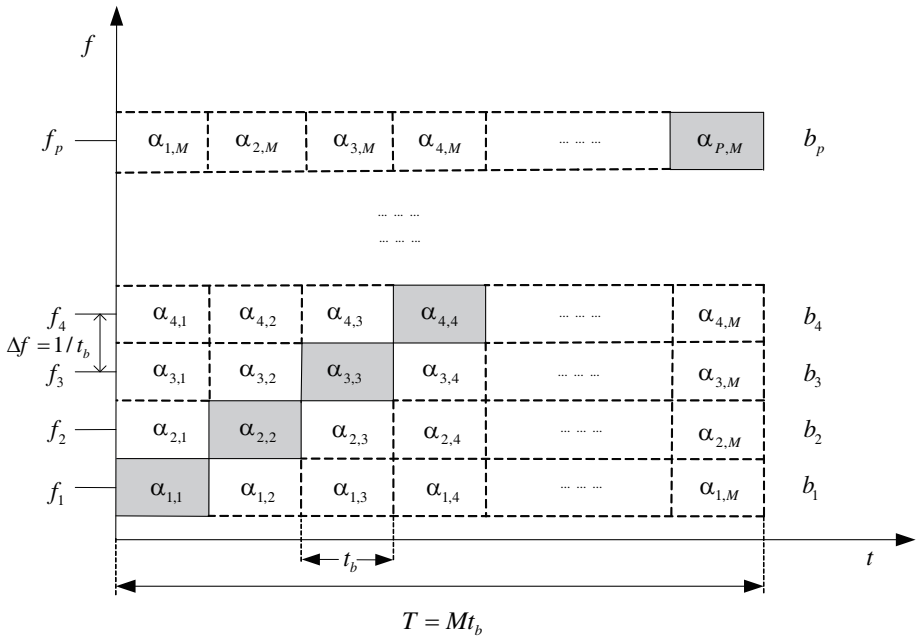

Figure 1. Time-frequency structure of the SCC-MCPC signal.

The dotted part is the original MCPC-OFDM signal, and the shaded part is the time-frequency diagram of SCC-MCPC signal.

Compared with OFDM signal, SCC-MCPC signal adds one-dimensional modulation, which makes the modulation mode of signal more flexible (phase). The SCC-MCPC signal is obtained by intercepting a part (shaded part) of each subcarrier in the MCPC signal at an intermediate interval. On this basis, due to the discontinuous nature of intermittent interference sampling, all subcarrier signals cannot be completely sampled, and different subcarriers are mutually orthogonal. Therefore, no matter how they are sampled in the time domain, the orthogonality between subcarriers can always be used to remove the sampled signal segment from the radar transmission signal.

3. ANTI-INTERFERENCE EFFECT OF SCC-MCPC SIGNAL WAVEFORM

To analyze the anti-interference effect of SCC-MCPC signal, the ambiguity function calculation formula can be obtained by combining the envelope expression (1) of SCC-MCPC signal:

$$\begin{aligned}
\chi(\tau, f_d) &= \int_{-\infty}^{+\infty} s(t)\, s^*(t+\tau)\, e^{j2\pi f_d t} dt \\
&= \int_{-\infty}^{+\infty} \sum_{n=1}^{P}\sum_{l=1}^{P} w_n \mu(t) \exp(j2\pi f_n t) \times w_l^* \mu^*(t+\tau) \exp[-j2\pi f_l (t+\tau)]\, e^{j2\pi f_d t} dt \\
&= \int_{-\infty}^{+\infty} \sum_{n=1}^{P}\sum_{l=1}^{P} w_n w_l^* \mu(t)\, w_l^* \mu^*(t+\tau) \exp[-j2\pi (f_n - f_l) t - j2\pi f_l \tau]\, e^{j2\pi f_d t} dt \\
&= \sum_{n=1}^{P}\sum_{l=1}^{P} w_n w_l^* \exp[-j2\pi f_l \tau] \int_{-\infty}^{+\infty} \mu(t)\, \mu^*(t+\tau) \exp[j2\pi (f_n - f_l) t]\, e^{j2\pi f_d t} dt \\
&= \sum_{l=1}^{P} w_n^2 \exp[-j2\pi f_l \tau] \int_{-\infty}^{+\infty} \mu(t)\, \mu^*(t+\tau)\, e^{j2\pi f_d t} dt
\end{aligned}$$

$$+\sum_{n=1}^{P}\sum_{l=1,l\neq n}^{P} w_n w_l^* \exp\left[-j2\pi f_l \tau\right] \int_{-\infty}^{+\infty} \mu\left(t\right) \mu^*\left(t+\tau\right) \exp\left[j2\pi\left(f_n - f_l\right) t\right] e^{j2\pi f_d t} dt \tag{7}$$

where $\chi(\tau v)$ is the ambiguity function of $s\left(t\right)$. Taking SCC-OFDM signals of 8 carriers as an example, compare the ambiguity function of LFM signals with the same bandwidth, as shown in Fig. 2 and Fig. 6.

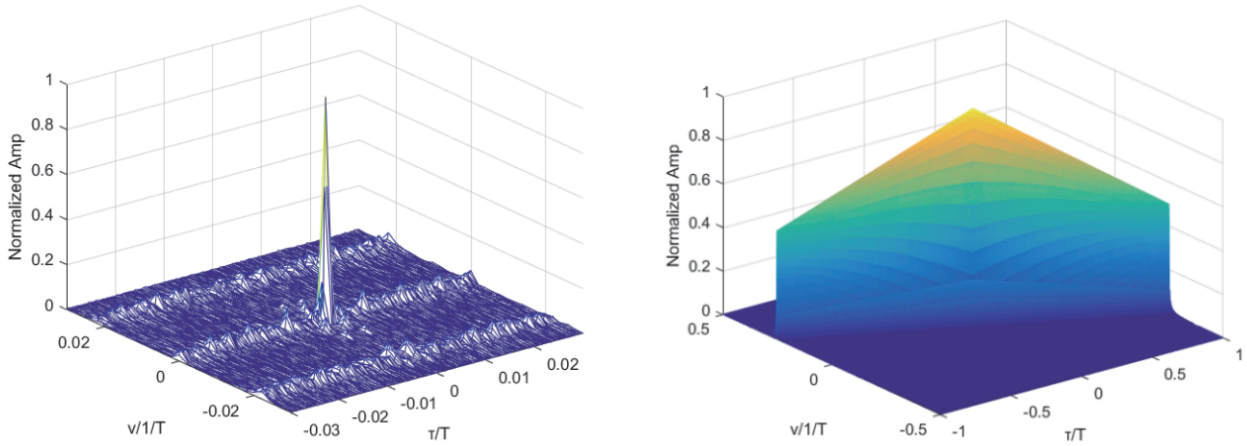

(a) (b)

Figure 2. Three-dimensional ambiguity figure. (a) SCC-MCPC, (b) LFM.

It can be seen from the figure that the energy of the signal ambiguity function modulated by the linear frequency modulation is relatively concentrated at the origin, and the figure is similar to a knife edge shape. The range Doppler coupling will make the range measurement inaccurate. The ambiguity function of SCC-MCPC signal modulated by chaotic phase encoding is ideal. The ambiguity function Doppler range Doppler plane is relatively flat; the amplitude fluctuation is small; and there is a single sharp peak at the origin. The sidelobe distribution outside the origin is relatively uniform and flat, and the overall appearance is close to the thumbtack. Compared with LFM signal, it has higher measurement accuracy and excellent target resolution.

4. ANALYSIS OF SCC-MCPC FRACTIONAL FOURIER TRANSFORM AND ECHO

4.1. Fractional Fourier Transform (FRFT) Analysis

FRFT introduces rotation factor α on the basis of Fourier transform to establish the connection between signal time domain and frequency domain. The basic idea is to use fractional Fourier transform to rotate and separate signals, so as to achieve the purpose of noise suppression. The separated signal recovers the original signal through the reverse rotation of the time-frequency plane. The p-order FRFT can be regarded as the time-domain and frequency-domain images of signals observed through different angles after the coordinate axis of the signal in the time-frequency domain rotates counterclockwise around the origin $\alpha = p\pi/2$. When the rotation angle is $\pi/2$, it is Fourier transform, as shown in Fig. 3.

The p order FRFT of the radar transmission signal is $s\left(t\right)$ defined as:

$$S\left(u\right) = \int_{-\infty}^{+\infty} K_p\left(t,u\right) s\left(t\right) dt \tag{8}$$

The Kernel function $K_p\left(t,u\right)$ is defined as:

$$K_p\left(t,u\right) \begin{cases} A_\alpha e^{i\pi\left(u^2\cot_\alpha - 2ut\csc\alpha + t^2\cot\alpha\right)} & \alpha \neq n\pi \\ \delta\left(t-\tau\right) & \alpha = 2n\pi \\ \delta\left(t+\tau\right) & \alpha = \left(2n+1\right)\pi \end{cases} \tag{9}$$

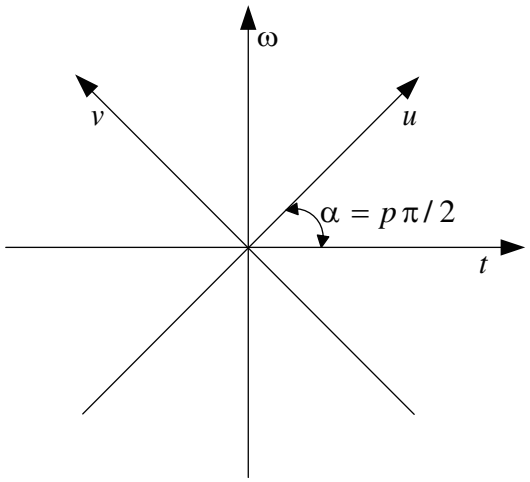

Figure 3. Fractional fourier domain (u, v).

In the above formula, $A_\alpha = \sqrt{1 - i\cot\alpha}$, $\alpha = p\pi/2$; τ is the delay, and n is an integer.

4.2. SCC-MCPC Fractional Fourier Transform Analysis

The selected p-order fractional Fourier domain should follow two principles: one is that the subcarrier signal has good aggregation, and the other is that there is min coupling between subcarriers. SCC-MCPC signal has phase mutation at the junction of signal symbols, which will cause discontinuity (aliasing) of signal spectrum, and the resulting spectrum leakage will interfere with fast Fourier transform (FFT) filtering. To solve this problem, this paper introduces the FRFT filtering method, which can reduce the effect of signal spectral leakage, improve the aggregation of subcarrier signals, reduce the coupling between subcarrier signals, make the subcarriers easier to separate in the frequency domain, and have higher filtering efficiency. The u domain after FRFT is divided into N equal length L, where N is the number of subcarriers. Calculate the sum of the energies of each L length region. When the variance between the energies of each region is the smallest, there is an optimal rotation order P. In the u domain, the SCC-MCPC signal of each L length is: $S_{\mathrm{Sub}i}(u) = \mathrm{rect}(u - (i-1)t_B)S(u)$, where t_B is the subcarrier pulse width. Using the ergodic algorithm, set the value interval of p at [0–2]. Calculate

$$\frac{1}{N-1}\sum_{i=1}^{N}\sqrt{\int_{-\infty}^{+\infty}|S_{\mathrm{Sub}i}(t)|^2\,dt - \frac{1}{N}\sum_{k=1}^{N}\int_{-\infty}^{+\infty}|S_{\mathrm{Sub}k}(t)|^2\,dt} \tag{10}$$

When the result is the smallest, P is the best rotation order. Under the parameter in Table 1, the optimal rotation order is obtained as 0.5.

Table 1. Simulation parameters of the scene.

Parameter	Value
Bandwidth	32 MHz
Carrier frequency	35 GHz
Pulse repetition period	1280 μs
Pulse width	128 μs
Subcarrier number	8
Chips number	512
Chips width	0.25 μs
Rotation order p	0.5

Under the parameters in Table 1, the comparison of FFT and FRFT of signals is shown in Fig. 4.

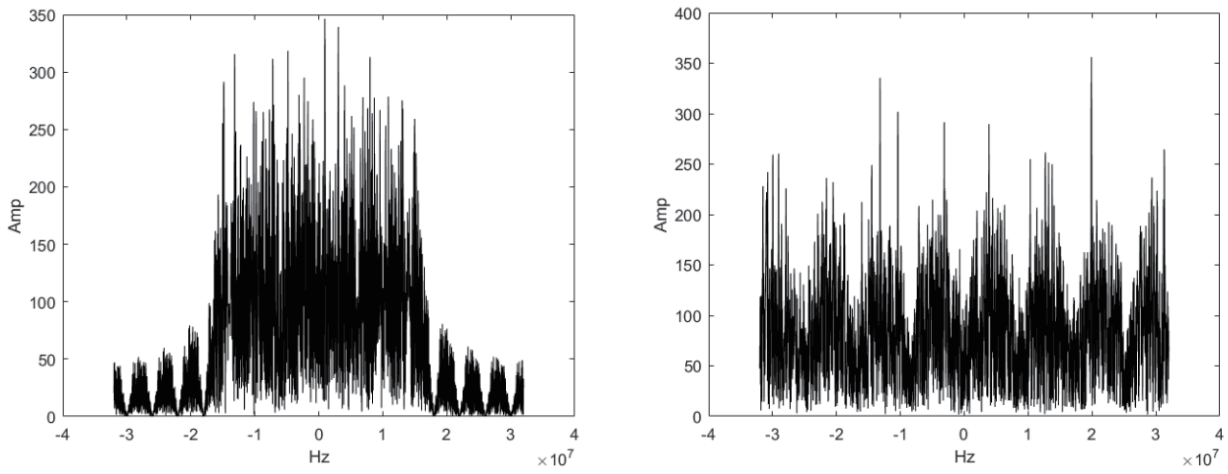

Figure 4. Different domains of transformation. (a) FFT transformation of SCC-MCPC signal. (b) FRFT transformation of SCC-MCPC signal.

It can be seen from the figure above that FRFT has higher coupling, stronger energy aggregation, lower filtering effect, lower signal coupling, and lower energy aggregation than the subcarriers in original FFT frequency domain, which makes it easier to filter and separate subcarriers.

4.3. SCC-MCPC Echo Pulse Compression Analysis

Usually, ISRJ jammer cannot replicate the whole radar signal. On this basis, combined with the nature of mutual orthogonality between subcarriers, it can be expected that after the pulse compression operation between subcarriers and echoes, different pulse compression results will be obtained. We judge whether the echo is interference by the pulse compression peaks of different subcarriers and echoes. The results of pulse compression can be expressed as follows:

$$S_{PC}(t) = \sum_{n=1}^{P} \int_{-\infty}^{+\infty} s(t) \operatorname{rect}(t-(n-1)t_B) s_R(t+\tau) d\tau \tag{11}$$

where P represents the number of subcarriers, $s_{PC}(t)$ the pulse compression result, t_B the duration of each subcarrier, and $s_R(t)$ the echo signal. In order to analyze the peak characteristics under different intermittent sampling disturbances, we assume that the echoes of four cases are received. The echo parameters are the same as in those in Table 1 and Table 2. The results of pulse compression for different echoes and subcarriers are shown in Fig. 5.

It can be seen that the number of peaks of pulse compression can determine whether the echo is a real target or an interference signal. In Fig. 5(a), when the echo is a real target, the number of peaks is the same as the number of subcarriers, and the peak heights are similar. In Figs. 5(b), (c), and (d), when the echo is a false target, the number of peaks is variable, and the height is inconsistent. This feature can be used to distinguish the real target from the interference.

5. ANTI INTERFERENCE ALGORITHM FLOW OF FRACTIONAL FOURIER TRANSFORM FILTER SUBCARRIER PULSE COMPRESSION

The echo signal processing flow of FRFT is shown in Fig. 6. It can be seen that in order to effectively remove the interference in the received echo, the method performs FRFT on the received echo signal,

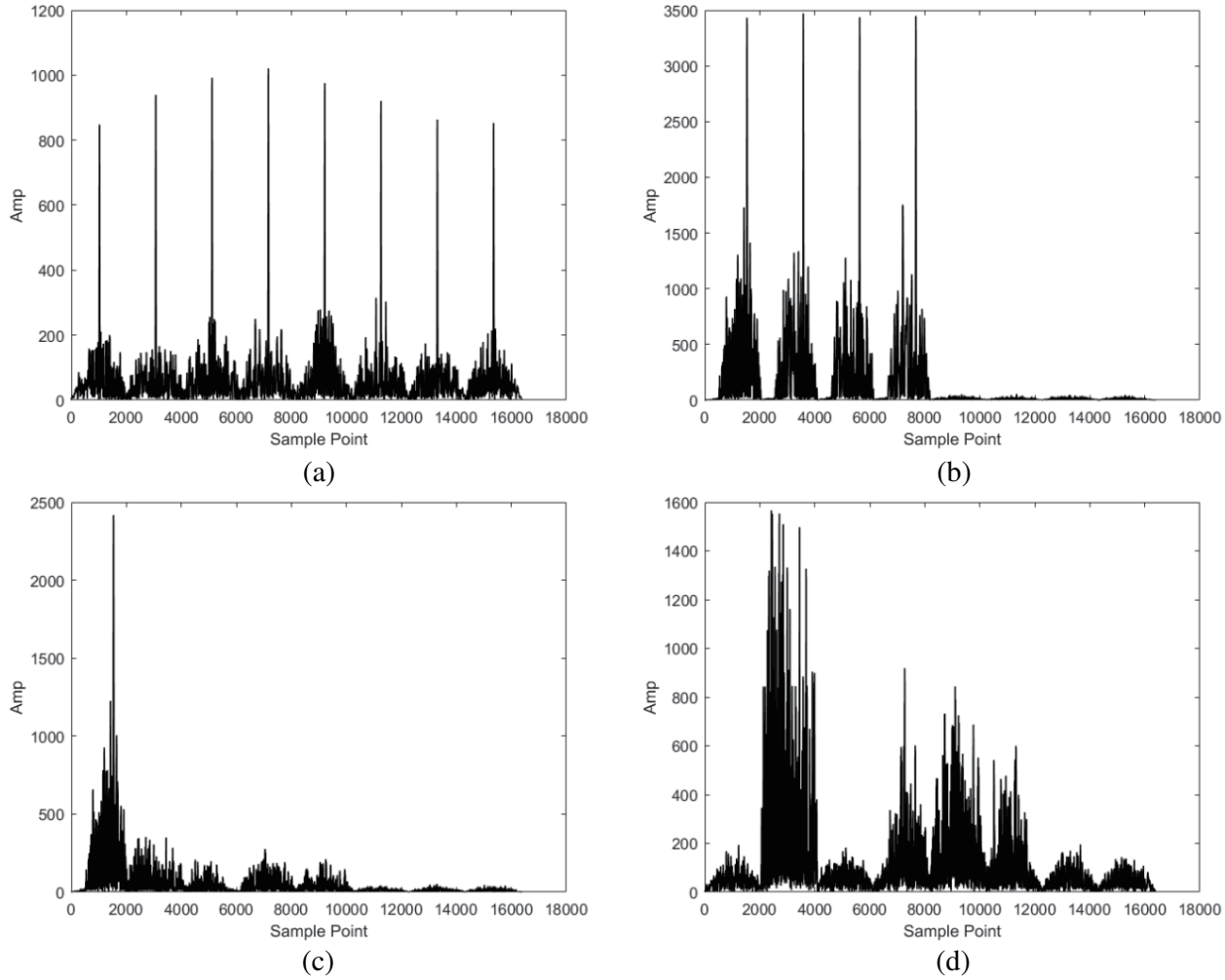

Figure 5. Comparison of different echo pulse compression. (a) Ture Target, (b) ISDJ, (c) ISPJ, (d) ISCJ.

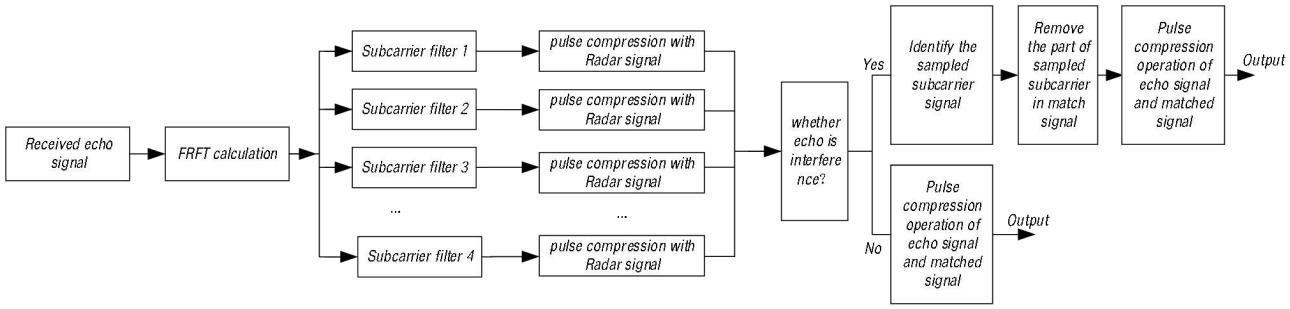

Figure 6. Flow chart of anti jamming signal of segmented pulse compression.

and then performs subcarrier filtering on the received signal. After frequency domain filtering, the subcarriers are separated, and then converted into time-domain subcarrier signals through fractional Fourier inverse transform. The difference between the subcarrier pulse compression results is analyzed by pulse compression of the subcarrier signal and the matching signal. The difference is used to separate the real target signal from the interference signal to achieve the purpose of suppressing interference.

Specifically, set the radar transmission signal as $s(t)$. Intermittent sampling signal of jammer is a

Table 2. Simulation parameters of the scene.

Parameter	Value
SJR (signal-jamming ratio)	−6 dB
SNR (signal to noise ratio)	3 dB
Iteration number	500
ISDJ slice width T_J	8 µs
ISDJ Number of slices H	4
ISDJ amplification factor A	8
ISPJ slice width T_J	8 µs
ISPJ forwarding times of each slice N	4
ISPJ delay coefficient α	1
ISPJ amplification factor B	5
ISCJ slice width T_J	8 µs
ISCJ delay coefficient α	4
ISCJ delay coefficient β	1
ISCJ amplification factor C	6

rectangular pulse train signal $s_j(t)$. The time width of each sampling pulse is τ_p, and the width of the intermittent sampling repetition period is T_p. The interference pulse can be expressed as:

$$s_j(t) = \text{rect}\left(\frac{t}{\tau_p}\right) \otimes \delta(t - nT_p) \tag{12}$$

Assuming that the jammer transmits this signal after sampling, and the delay τ, then the intermittent sampling and transmitting jamming signal is: $s_{ISRJ}(t) = s(t-\tau)s_j(t-\tau)$.

The received echo signal is:

$$s_{\text{Echo}}(t) = s_R(t) + s_{\text{ISRJ}}(t) + n(t) \tag{13}$$

In formula (13), $s_R(t)$ is the real echo signal of the scattering target at distance R; $s_{ISRJ}(t)$ is the ISRJ interference; and $n(t)$ is the environmental noise. Then the signal after fractional Fourier transform processing can be expressed as: $S_{F\text{RFT}}(u) = \int_{-\infty}^{+\infty} K_p(t,u)\, s_{\text{Echo}}(t)\, dt$. Subcarrier filtering processing is performed on the signal in the u domain to obtain the i-th subcarrier signal $S_{\text{Sub}i}(u) = \text{rect}(t-(n-1)t_B)S_{\text{FRFT}}(u)$. Then fractional Fourier inverse transform processing is performed on the separated subcarrier signal to obtain the time-domain expression of the K-th subcarrier as BBBB. Then pulse compression processing is performed on the subcarrier signal and radar transmission signal, respectively. The pulse compression results are obtained after summing the processing results:

$$\tau_{Subi}(t) = \sum_{l=1}^{P} \text{rect}(t - i * t_B) \int_{-\infty}^{+\infty} S_{\text{Sub}i}(t)\, S(t+\tau) d\tau \tag{14}$$

t_B is the subcarrier pulse width. According to the under sampling theory of the jammer and the principle that the signal subcarriers are orthogonal to each other proposed in this paper, it can be seen that if the echo signal is a real target, the amplitude values of all the subcarrier pulse compression results are highly similar; if the echo signal is a false target, the output of the matching result between the sampled subcarrier signal and nonsampled subcarrier signal is close to 0.

Considering the influence of noise and other interference factors in the environment, set the maximum value of subcarrier pulse compression output as $MAX[\tau_{Subi}(t)]$ and μ as the difference coefficient. If the pulse compression output $\tau_{Subi}(t)$ of other subcarriers is greater than $\mu MAX[\tau_{Subi}(t)]$, the echo signal is considered to be a real target. As long as one subcarrier pulse compression output

does not meet the conditions, the echo signal is considered to have received ISRJ. Thus interference suppression becomes a judgment problem

$$\left.\begin{array}{ll} \tau_{Subi}(t) \leq \mu MAX, & \text{Ture Target} \\ \text{else}, & \text{False Target} \end{array}\right\} \tag{15}$$

When judging that the signal receives ISRJ interference, remove the subcarriers whose pulse compression output exceeds A to remove ISRJ interference. Through the joint design of radar transmission waveform and fractional Fourier filter, the purpose of suppressing intermittent sampling interference is finally achieved.

6. SIMULATION ANALYSIS (PERFORMANCE ANALYSIS OF ANTI INTERMITTENT SAMPLING INTERFERENCE)

To verify the antiintermittent sampling interference effect of the designed method, this section uses simulation experiments to simulate the antiintermittent sampling interference effect of the method. The original radar transmission signal is jammed by three jamming methods, namely, ISDJ, ISPJ, and ISCJ. Based on the simulation, the anti-interference effect of the method proposed in this paper is verified.

6.1. Performance Analysis of Anti-Replication Forwarding Interference

Under the same sampling rate and intermittent sampling period, different jamming strategies will produce different jamming effects on signals. After the signal is sampled by the ISDJ, the sampling slice is amplified and forwarded. The sampling time is equal to the forwarding time. After the receiver compresses the echo signal, a single false target jamming will be formed. The time domain expression is:

$$s_{ISDJ}(t) = A\sum_{h=0}^{H} \text{rect}\left(\frac{t-(2h+1)T_J}{T_J}\right) s(t-T_J) \tag{16}$$

where H is the number of slices, T_J the width of slices, and $s(t)$ the intercepted radar transmitted signal.

The ISPJ replicates and amplifies the sampling slice and then forwards it for many times. It replicates multiple intercepted signals as interference slices in a continuous time. The interference slices are amplified and then retransmitted for many times. After the pulse compression processing, it will form continuous multiple false target string interference. Its time domain expression is:

$$s_{ISPJ}(t) = B\sum_{h=1}^{H}\sum_{n=1}^{N} \text{rect}\left(\frac{t-\alpha(h,n)T_J}{T_J}\right) s(t-nT_J) \tag{17}$$

where N is the forwarding times of each slice, and $\alpha(h,n) = (h-1)(N+1)+n$ is the delay coefficient corresponding to the nth forwarding of the hth slice.

ISCJ replicates multiple resampling slices in a continuous time. After amplification, different copied slices are spliced and forwarded after a period of delay. After pulse compression, multiple continuous false targets will be formed. Its time domain expression is:

$$s_{ISCJ}(t) = C\sum_{h=1}^{H}\sum_{n=1}^{H-h+1} \text{rect}\left(\frac{t-\alpha(h)T_J-\beta(h,n)T_J}{T_J}\right) s(t-\beta(h,n)T) \tag{18}$$

where $\alpha(h) = h(h+1)/2-1$ is the delay coefficient corresponding to the hth slice, and $\beta(h,n) = n(n+1)/2+h(n-1)$ is the delay coefficient corresponding to the nth slice.

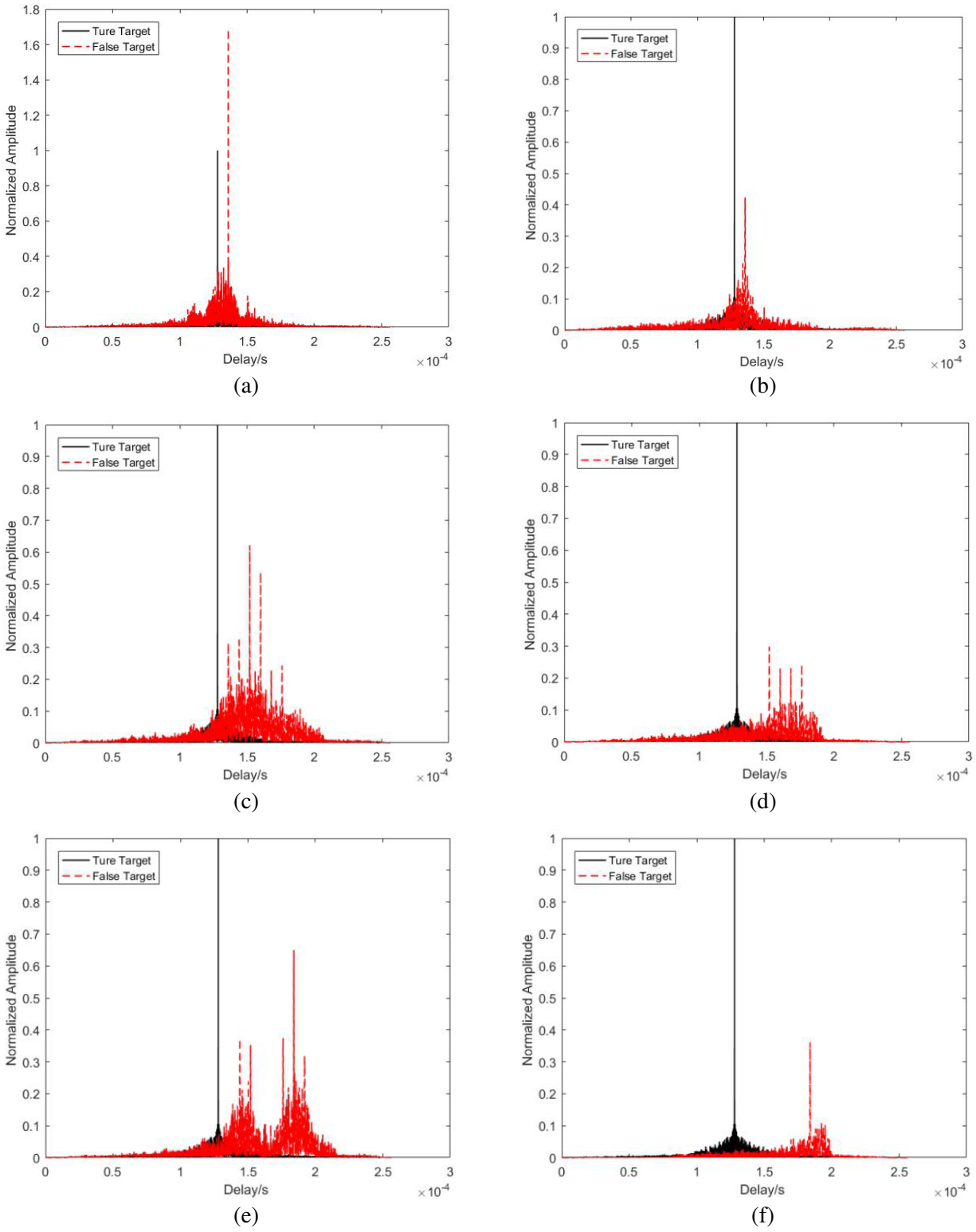

Figure 7. Different Intermittent Sampling Interference Suppression. (a) Before ISDJ suppression. (b) After ISDJ suppression. (c) Before ISPJ suppression. (d) After ISPJ suppression. (e) Before ISCJ suppression. (f) After ISCJ suppression.

6.2. Different Jamming and Forwarding Forms Will Produce Different Jamming and False Target Effects

According to the interference suppression scheme proposed in this paper, different interference strategies are simulated to verify the suppression effect of this method. The simulation results are shown in Fig. 7. The simulation scenario parameter settings are shown in Table 2, and the other parameters are the same as those in Table 1. The antiintermittent sampling interference processing flow is shown in Fig. 7.

After data normalization, it can be seen from Fig. 7(a) and Fig. 7(b) that when ISDJ is not subject to interference suppression processing, ISDJ pulse compression produces suppression and deception effects on real targets, which makes it difficult to distinguish real targets. After the interference suppression of the method proposed in this paper, the single false target interference is suppressed, and its pulse pressure height decreases significantly. It can be seen from Figs. 7(c) and 7(d) that continuous false targets are generated after ISPJ pulse compression. After interference suppression by the method proposed in this paper, some false targets are completely suppressed, and the pulse pressure height of other false targets decreases slightly. It can be seen from Figs. 7(e) and (f) that after the ISCJ pulse compression, two consecutive jamming target strings are generated. After the proposed method of interference suppression, one of the consecutive jamming target strings is suppressed, and the height

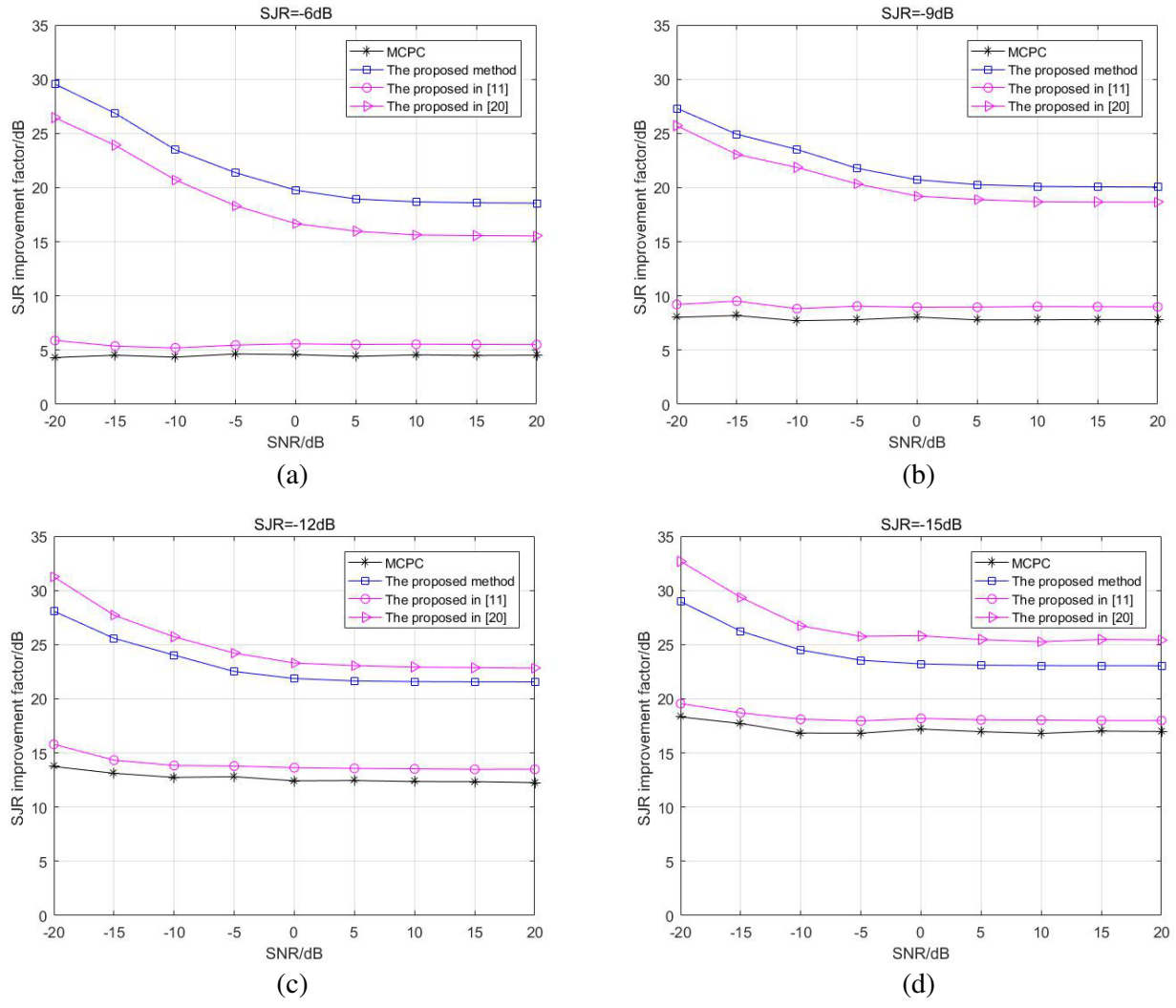

Figure 8. Simulation comparison of SJR improvement factors under different SNRs and SJRs. (a) SJR = −6 dB, (b) SJR = −9 dB, (c) SJR = −12 dB, (d) SJR = −15 dB.

of the other jamming target string is also significantly reduced. The reason that the method cannot completely suppress the interference is that the jammer is randomly sampled, and the spectrum of the intercepted signal during the sampling process may be exactly at the junction of the two subcarrier spectra, so the interference cannot be completely suppressed. The simulation results show that the method in this paper can significantly suppress three kinds of ISRJ.

7. COMPARISON EXPERIMENT

We compare the proposed method with the methods in [11] and [20], Since paper [20] has set the specific scenario, we assume that the parameters of Doppler frequency shift compensation and time delay are known. In order to more intuitively reflect the improvement of SJR improvement factor, we also added MCPC signal under the same parameter conditions as a comparison. The input values of the matched filter SJR are -6 dB, -9 dB, -12 dB, and -15 dB, respectively. The simulation parameters of the input signal are as follows: the carrier frequency is 35 GHz; the signal bandwidth is 32 MHz; the pulse repetition period is 1280 µs; the sampling rate is 64 MHz; and the pulse width is 128 µs. The results of 500 Monte Carlo experiments are shown in Fig. 8.

It can be seen from Fig. 8 that under the same parameter settings and different SJRs and SNRs, the SCC-MCPC signal anti-interference method proposed in this paper is superior to the time-frequency random coded multicarrier chaotic phase code (TFRC-MCPC) signal anti-interference method proposed in [11]. The SJR improvement factor of SCC-MCPC signal is $5 \sim 12$ dB higher than that of TFRC-MCPC signal. It is 6–12 dB higher than the traditional MCPC signal.

For the method proposed in [20], the SJR improvement factor of the method proposed in this paper is on average 3.01 dB and 1.52 dB higher than that of [20] when the input SJR $= -6$ dB and SJR $= -9$ dB, and on average 1.71 dB and 2.58 dB lower when the input SJR $= -12$ dB and SJR $= -15$ dB. The reason for this is that when the input SJR is low, paper [20] uses Doppler frequency shift compensation to compensate the frequency shift of the noise in the interference signal and the interference signal together, which can filter the noise and the interference signal together. However, the method in this paper can only remove the interference signal and cannot filter the noise generated with the interference signal. Therefore, this method is better than [20] for larger input SJR and worse than [20] for smaller input SJR. Due to the limitation of usage scenarios in paper [20], this method is more universal and better than paper [20] in general.

8. CONCLUSION

According to the principle of time domain ISRJ discontinuity and the idea of mutual Cover between subcarriers, an ISRJ suppression method based on FRFT filter segmented pulse compression is proposed. This method uses chaotic sequences to encode the MCPC signal in time domain and then intercepts the chip lengths of different subcarriers of the MCPC with equal spacing to generate SCC-MCPC signal. On this basis, the real target and interference are distinguished according to the characteristics of the different peaks of the echo signal. Then the interference echoes are removed by filtering different subcarriers of echoes. Compared with the prior art, ISRJ parameter estimation is not required and is easy to implement. Theoretical analysis and simulation results show that the method can effectively suppress three typical ISRJ interferences with strong anti-interference performance, which provides a new solution for radar anti-interference.

ACKNOWLEDGMENT

This work was supported in part by the Changsha Natural Science Foundation (kq2014111) and Seed Fund of Research and Development Center for Multi-Sensor Intelligent Detection and Recognition Technology (ZZJ202103-02).

REFERENCES

1. Wang, X. S., J. Liu, W. Zhang, Q. Fu, Z. Liu, and X. Xie, "Mathematic principles of interrupted-sampling repeater jamming (ISRJ)," *Science in China Series F: Information Science*, Vol. 50, No. 1, 113–123, 2007.
2. Sparrow, M. J. and J. Cikalo, "ECM techniques to counter pulse compression radar: US, Patent 7081846[P]," 2006.
3. Feng, D. J., H. M. Tao, and Y. A. Yang, "Jamming de-chirping radar using interrupted-sampling repeater," *Science China Information Sciences*, Vol. 10, No. 54, 2138–2146, 2011.
4. Li, C. Z., W. M. Su, H. Gu, C. Ma, and J. L. Chen, "Improved interrupted sampling repeater jamming based on DRFM," *2014 IEEE International Conference on Signal Processing, Communications and Computing, ICSPCC 2014*, No. 6986193, 254–257, 2014.
5. Liu, M., S. Tao, and Q. Chen, "Countermeasure for interrupted-sampling repeater jamming based on fractional Fourier transformation," *MATEC Web of Conferences*, Vol. 232, No. 03037, 2018.
6. Wang, Z. J, W. B. Yu, and Z. J. Yu, "Neural network-guided sparse recovery for interrupted-sampling repeater jamming suppression," *International Journal of Antennas and Propagation*, Vol. 2021, 2021.
7. Zhou, K., D. Li, and S. Quan, "SAR waveform and mismatched filter design for countering interrupted sampling repeater jamming," *IEEE Transactions on Geoscience and Remote Sensing*, Vol. 60, 2022.
8. Liu, Y., Q. Zhang, and Z. Liu, "An anti-jamming method against interrupted sampling repeater jamming based on compressed sensing," *Sensors*, Vol. 22, No. 2239, 2022.
9. Duan, J., L. Zhang, and Y. F. Wu, "Interrupted-sampling repeater jamming suppression with one-dimensional semi-parametric signal decomposition," *Digital Signal Processing: A Review Journal*, Vol. 127, 2022.
10. Lu, L. and M. G. Gao, "An improved sliding matched filter method for interrupted sampling repeater jamming suppression based on jamming reconstruction," *IEEE Sensors Journal*, Vol. 22, No. 10, 9675–9684, 2022.
11. Li, J., X. Luo, X. Duan, W. Wang, and J. Ou, "A novel radar waveform design for anti-interrupted sampling repeater jamming via time-frequency random coded method," *Progress In Electromagnetics Research M*, Vol. 98, 89–99, 2020.
12. Zhou, C., Q. Liu, and X. Chen, "Parameter estimation and suppression for DRFM-based interrupted sampling repeater jammer," *IET Radar, Sonar and Navigation*, Vol. 12, No. 1, 56–63,2018.
13. Zhou, K., D. Li, Y. Su, and T. Liu, "Joint design of transmit waveform and mismatch filter in the presence of interrupted sampling repeater jamming," *IEEE Signal Processing Letters*, 2020.
14. Xiong, W., G. Zhang, and W. Liu, "Efficient filter design against interrupted sampling repeater jamming for wideband radar," *Eurasip Journal on Advances in Signal Processing*, Vol. 2017, No. 1, No. 9, 2017.
15. Chen, J., W. Wu, S. Xu, Z. Chen, and J. Zou, "Band pass filter design against interrupted-sampling repeater jamming based on time-frequency analysis," *IET Radar, Sonar and Navigation*, Vol. 13, No. 10, 1646–1654, 2019.
16. Wei, Y., Z. Lu, G. Yuan, Z. Fang, and Y. Huang, "Sparsity adaptive matching pursuit detection algorithm based on compressed sensing for radar signals," *Sensors (Switzerland)*, Vol. 17, No. 5, 2017.
17. Zhao, Y., C. Shang, Z. Han, N. Han, and H. Xie, "Fractional fourier transform and compressed sensing adaptive countering smeared spectrum jamming," *Dianzi Yu Xinxi Xuebao/Journal of Electronics and Information Technology*, Vol. 41, No. 5, 1047–1054, 2019.

18. Fang, B., and G. Huang, and J. Gao, "Sub-nyquist sampling and reconstruction model of LFM signals based on blind compressed sensing in FRFT domain," Vol. 34, No. 2, 419–439, 2015.
19. Zhang, J., H. Mu, S. Wen, Y. Li, and H. Gao, "Anti-intermittent sampling repeater jamming method based on LFM segmented pulse compression," *Dianzi Yu Xinxi Xuebao/Journal of Electronics and Information Technology*, Vol. 41, No. 7, 1712–1720, 2019.
20. Zhang, Y., Y. S. Wei, and L. Yu, "Interrupted sampling repeater jamming recognition and suppression based on phase-coded signal processing," *Signal Processing*, Vol. 198, 2022.
21. Li, J., Q. Deng, J. P. Ou, and W. Wang, "Research on random redundant multi-carrier phase code signal against ISRJ based on MIMO radar," *Progress In Electromagnetics Research M*, Vol. 110, 97–107, 2022.
22. Bultheel, A. and H. E. M. Sulbaran, "Computation of the fractional Fourier transform," *Applied and Computational Harmonic Analysis*, Vol. 16, No. 3, 182–202, 2004.
23. Atakishiyev, N. M., L. E. Vicent, and K. B. Wolf, "Continuous vs. discrete fractional Fourier transform," *Journal of Computational and Applied Mathematics*, Vol. 107, No. 1, 73–95, 1999.
24. Li, J., M. Liu, J. P. Ou, and W. Wang, "A novel radar waveform design for suppressing autocorrelation side-lobe based on chaotic and single fusion encoding method," *Progress In Electromagnetics Research M*, Vol. 111, 77–88, 2022.